Pulsed-Nuclear-Magnetic-Resonance Study of GdP, LaP:Gd, and LuP:Gd: Dynamics of a Heisenberg Paramagnet*

S. M. Myers and A. Narath
Sandia Laboratories, Albuquerque, New Mexico 87115
(Received 16 October 1972)

Measurements of the magnetic field dependences of T_1 and T_2 for ^{31}P nuclei in GdP at temperatures $T \gg T_N$ are reported. These relaxation times are shown to yield the Fourier transform of the sum of two electronic-spin correlation functions. This is the first case where these functions have been determined from nuclear magnetic resonance (NMR), and a fairly good fit to a theoretical spectrum is achieved. Comparison of the fit parameters with results of previous NMR-shift measurements gives information about the ranges of the Gd-P hyperfine interaction and the Gd-Gd exchange interaction. A more detailed characterization of the hyperfine coupling is obtained from the ^{31}P spectra in LaP and LuP containing dilute substitutional Gd. These spectra were taken at temperatures ≤ 4 °K and magnetic fields near 100 kOe. The resulting saturation of the Gd spins makes exchange effects unimportant, thereby simplifying interpretation of the data. Two peaks are resolved. One is assigned to ^{31}P nuclei having one nearest-neighbor Gd, the other to ^{31}P nuclei having none. The combined data indicate that the nearest-neighbor hyperfine coupling accounts for $(78 \pm 5)\%$ of the resonance shift in GdP, the remainder being due to longer-range interactions. Appreciable anisotropy is observed in the hyperfine interaction. Finally, consistency among all the results is obtained if the Gd-Gd exchange is assumed to be next-nearest neighbor only.

I. INTRODUCTION

We have made a detailed study of the magnetic properties of GdP via the transient nuclear magnetic resonance (NMR) of ^{31}P.[1] Measured were the magnetic field dependences of the longitudinal and transverse nuclear-spin relaxation times T_1 and T_2. The Gd-^{31}P hyperfine coupling makes these parameters sensitive to the Gd^{3+} electronic-spin fluctuations. As will be discussed, the results yield the Fourier transform with respect to time of the sum of the electronic-spin autocorrelation function and a pair correlation function. These functions characterize in part the time evolution of the electronic-spin system. Such detailed information has previously been available only from inelastic-neutron-scattering experiments, which yield the Fourier transform with respect to both space and time.[2] Furthermore, when the present data are combined with previous resonance-shift data[3] they provide information on the ranges of the Gd-Gd exchange interaction and the Gd-P hyperfine coupling. This is a consequence of the quadratic dependence of the relaxation times on the hyperfine and exchange interactions, which contrasts with the linear sums over these interactions which determine the resonance shift. Also obtained were ^{31}P spectra in LaP and LuP containing dilute Gd, which permitted a still more detailed characterization of the hyperfine interaction from the satellites associated with P-Gd nearest neighbors.

The motivation for this work was twofold. First, GdP is especially well suited to the field-dependence study because the applied magnetic field can be varied from values much smaller to much larger than the exchange field acting on the Gd spins. In the second place, the GdP work is part of a systematic study of the rare-earth (RE) monophosphide series.[4,5] The RE-RE exchange interaction and the RE-P hyperfine coupling in these intermetallic compounds are of interest because they have been thought to procede via conduction-electron polarization. In particular, the range of these couplings should reflect the size of the polarization cloud surrounding the localized spin on a RE ion.

The RE phosphides have the NaCl structure and are metallic.[6] GdP differs from the other compounds of this series in that the Gd^{3+} $4f$ shell is half filled, with $J = S = \frac{7}{2}$ and $L = 0$. The resulting spherical symmetry of the ionic wave function should result in crystal field effects being negligible and the Gd-Gd exchange interaction being isotropic. The isotropy of the exchange has been confirmed for GdP from high-temperature electron-paramagnetic-resonance (EPR) linewidth measurements by Bartkowski.[7] The only anisotropy in the Gd-Gd coupling is therefore due to classical dipolar fields, which are smaller than the exchange fields by about an order of magnitude. GdP orders antiferromagnetically at 15 °K,[8] and has a Curie-Weiss temperature of -22.4 ± 2 °K.[3] A molecular field treatment based on these values yields a next-nearest-neighbor exchange interaction which is about 4 times larger than the nearest-neighbor exchange.[9] The analogs LaP and LuP are nonmagnetic, having, respectively, an empty and a filled

$4f$ shell. Their conduction and valence bands should be very nearly the same as for GdP, since the configurations of the outer s and d valence shells are presumably identical. The lattice constants are 6.025 Å for LaP, 5.723 Å for GdP, and 5.533 Å for LuP, [10] exhibiting a monotonic variation with RE atomic number. Hence, LaP and LuP containing dilute Gd should be well suited to the study of the Gd-P coupling.

In Sec. II the relevant theory is reviewed and extended to cover the present work. In Sec. III the experimental procedure is described, and in Sec. IV the results are analyzed. The conclusions follow in Sec. V.

II. THEORY

The behavior of the coupled ^{31}P-nuclear-spin–Gd^{3+}-electronic-spin system is governed by three interactions: the Gd-Gd exchange, the Gd-lattice coupling, and the Gd-P hyperfine interaction. The exchange interaction is the largest, and it determines the fluctuation spectrum of the Gd spins. The Gd-lattice relaxation, whose rate is known from EPR saturation studies of dilute Gd in LaP, [11] is some 4 orders of magnitude slower than the Gd-Gd exchange. It is important, however, because it maintains thermal equilibrium between the Gd-spin system and the lattice. The Gd-P hyperfine coupling causes relaxation of the ^{31}P nuclear spins, but does not significantly affect the Gd electronic spins. Finally, as will be discussed in Sec. IV, nuclear-spin relaxation not associated with the Gd-P coupling is entirely negligible.

The situation outlined above can be described in terms of the Hamiltonian

$$\mathcal{H} = \mathcal{H}_e + \mathcal{H}_N , \tag{2.1}$$

where

$$\mathcal{H}_e = \frac{1}{2}\sum_{i\neq j} \mathcal{J}_{ij}\vec{S}_i\cdot\vec{S}_j + g\mu_B H\cdot\sum_i \vec{S}_i \tag{2.2}$$

and

$$\mathcal{H}_N = \vec{I}_N\cdot\sum_i \overleftrightarrow{A}_i\cdot\vec{S}_i - \gamma_N\hbar\vec{H}\cdot\vec{I}_N . \tag{2.3}$$

Here $\vec{S}$ is the total electronic spin on the Gd ion, $\mathcal{J}$ is twice the exchange integral, $\vec{H}$ is the applied field, $\vec{I}_N$ is the nuclear spin, $\overleftrightarrow{A}_i$ is the Gd-P hyperfine coupling tensor due to a Gd ion in the ith neighboring position surrounding the P sites, and γ_N is the nuclear gyromagnetic ratio. The exchange has been written as an isotropic interaction for reasons given in Sec. I, while the more general form for the hyperfine interaction has been used. It is valid to express Eq. (2.3) in terms of an effective field acting on the nuclei. Thus one has

$$\mathcal{H}_N = -(\vec{h}+\vec{H})\cdot\gamma_N\hbar\vec{I}_N , \tag{2.4}$$

where

$$\vec{h} = -(\gamma_N\hbar)^{-1}\sum_i \overleftrightarrow{A}_i\cdot\vec{S}_i . \tag{2.5}$$

The Gd-lattice interaction is taken account of by assuming the electronic-spin system to remain in thermal equilibrium with the lattice, i.e., by using the density operator $e^{-\mathcal{H}_e/k_BT}$ to characterize the population of its levels.

The nuclear-spin longitudinal relaxation time T_1 and the transverse relaxation time T_2 are given by [12]

$$T_1^{-1} = \tfrac{1}{2}\gamma_N^2\int_{-\infty}^{+\infty}[\langle h^x(t)h^x(0)\rangle + \langle h^y(t)h^y(0)\rangle]e^{-i\omega_N t}\,dt \tag{2.6}$$

and

$$T_2^{-1} = \tfrac{1}{2}T_1^{-1} + \tfrac{1}{2}\gamma_N^2\int_{-\infty}^{+\infty}\langle h^z(t)h^z(0)\rangle dt . \tag{2.7}$$

Here z is the direction of the applied field, ω_N is the NMR frequency, which may be set to zero since it is much smaller than the electronic-spin-fluctuation rate, and the brackets $\langle\rangle$ indicate an ensemble average. Substitution of Eq. (2.5) into Eqs. (2.6) and (2.7) then relates the measured parameters T_1 and T_2 to the time evolution of the electronic-spin system. However, a considerable simplification can be achieved by first noting several facts.

The first point is that it is probably an excellent approximation to take the hyperfine interaction to be axially symmetric about the unit vector $\hat{r}$ between the ^{31}P nucleus and the Gd ion. Indeed, the part of the coupling due to classical dipolar fields obeys this condition. Furthermore, the symmetry of the lattice demands that it hold for the entire nearest-neighbor interaction, which will be the one of primary interest here. Equation (2.5) may then be written

$$\vec{h} = (\gamma_N\hbar)^{-1}\sum_i\{A_i\vec{S}_i + \mathfrak{a}_i[\vec{S}_i - 3(\hat{r}_i\cdot\vec{S}_i)\hat{r}_i]\} , \tag{2.8}$$

where A_i gives the magnitude of the isotropic coupling to a given Gd ion and $\mathfrak{a}_i$ characterizes the corresponding anisotropic part. The sign convention for A_i and $\mathfrak{a}_i$ has arbitrarily been chosen to give positive values for these parameters in the present experiment. (Note that the electronic magnetic moment is antiparallel to $\vec{S}$.) In the particular case of the classical dipolar interaction one has

$$A_i/\gamma_N\hbar = 0 \tag{2.9}$$

and

$$\mathfrak{a}_i/\gamma_N\hbar = g\mu_B/r_i^3 . \tag{2.10}$$

Several properties of the electronic-spin-correlation functions will permit further simplification. To obtain these properties requires precise definitions of the time-dependent spin operator and of the ensemble average. One has

$$\vec{S}(t) \equiv e^{it\mathcal{H}_e/\hbar}\vec{S}\,e^{-it\mathcal{H}_e/\hbar} \tag{2.11}$$

and

$$\langle O\rangle \equiv \mathrm{Tr}(O e^{-\mathcal{H}_e/k_BT})/\mathrm{Tr}\, e^{-\mathcal{H}_e/k_BT}\,, \tag{2.12}$$

which becomes in the high-temperature limit

$$\langle O\rangle = \mathrm{Tr}O/\mathrm{Tr}1\,, \tag{2.13}$$

where O is any operator. From Eqs. (2.2), (2.11), and (2.13) it can then be shown that

$$\langle S_i^x(t)S_j^y(0)\rangle + \langle S_i^y(t)S_j^x(0)\rangle = 0\,, \tag{2.14}$$

$$\langle S_i^z(t)S_j^z(0)\rangle_{H^z} = \langle S_i^z(t)S_j^z(0)\rangle_{H^z=0}\,, \tag{2.15}$$

and

$$\langle S_i^x(t)S_j^x(0)\rangle = \langle S_i^y(t)S_j^y(0)\rangle = \langle S_i^z(t)S_j^z(0)\rangle\cos\omega_0 t\,, \tag{2.16}$$

where

$$\omega_0 = g\mu_B H^z/\hbar\,. \tag{2.17}$$

Equations (2.15) and (2.16) indicate that in the high-temperature limit the spin fluctuations along the applied magnetic field are independent of the magnitude of that field, but that the transverse fluctuations are modulated at the electronic Larmor precession frequency. These two results are central to the interpretations presented in this paper. They depend specifically on the commutator of the exchange and Zeeman terms in the electronic Hamiltonian being zero. This is true for the isotropic exchange given in Eq. (2.2), but it may not hold when the exchange interaction is anisotropic. Hence, the present work cannot be applied indiscrimately to systems in which orbital contributions to the magnetic moment are important.

The final simplification will be to make two assumptions: first, that the Gd-P hyperfine interaction is nearest-neighbor only; and second, that the Gd-Gd exchange is next-nearest neighbor only. The former is an obvious first guess for the NaCl structure, while the latter is suggested by a molecular field treatment of the Néel and Curie–Weiss temperatures.[9] However, unlike Eqs. (2.8) and (2.14)–(2.16), these assumptions are open to question. Their validity will be judged by comparison with the experimental results. We may then divide the face-centered-cubic lattice of Gd ions into four interpenetrating simple-cubic lattices, each of which has zero coupling to the other three. A given ^{31}P nucleus is hyperfine-coupled to two nearest Gd neighbors in three of the four simple-cubic arrays; a total of six hyperfine couplings.

When all of the above considerations are included, Eqs. (2.6) and (2.7) become

$$\begin{aligned}T_1^{-1} = {}& \hbar^{-2}[12A_1^2 - 12\alpha_1^2 \\ & + 18\alpha_1^2(\sin^4\alpha+\sin^4\beta+\sin^4\gamma)] \\ & \times\int_0^\infty [\langle S_1^x(t)S_1^x(0)\rangle + \langle S_1^x(t)S_2^x(0)\rangle]\cos\omega_0 t\, dt \\ & + 18\hbar^{-2}\alpha_1^2(2-\sin^4\alpha-\sin^4\beta-\sin^4\gamma) \\ & \times\int_0^\infty [\langle S_1^z(t)S_1^z(0)\rangle + \langle S_1^z(t)S_2^z(0)\rangle]\, dt\end{aligned} \tag{2.18}$$

and

$$\begin{aligned}T_2^{-1} = {}& \tfrac{1}{2}T_1^{-1} + \hbar^{-2}[6A_1^2 - 6\alpha_1^2 \\ & + 18\alpha_1^2(\cos^4\alpha+\cos^4\beta+\cos^4\gamma)] \\ & \times\int_0^\infty [\langle S_1^z(t)S_1^z(0)\rangle + \langle S_1^z(t)S_2^z(0)\rangle]\, dt \\ & + 18\hbar^{-2}\alpha_1^2(1-\cos^4\alpha-\cos^4\beta-\cos^4\gamma) \\ & \times\int_0^\infty [\langle S_1^z(t)S_1^z(0)\rangle + \langle S_1^z(t)S_2^z(0)\rangle]\cos\omega_0 t\, dt\,,\end{aligned} \tag{2.19}$$

where α, β, and γ are the angles between the applied field direction z and the three crystalline axes, spins 1 and 2 are understood to be on next-nearest-neighbor Gd sites, and A_1 and α_1 are the nearest-neighbor hyperfine-coupling parameters. It should be stressed that the only field dependence in these equations is contained explicitly in the factor $\cos\omega_0 t$. In the low-field limit where $\omega_0 = 0$, and in the absence of pair-correlation effects [i.e., $\langle S_1^z(t)S_2^z(0)\rangle = 0$], these results become very similar to those obtained previously by Moriya.[13]

The physical significance of the formal development presented above can be seen more clearly by considering the case where the applied magnetic field is along the [100] crystalline axis. In Eq. (2.18) this corresponds to $\alpha = 0$ and $\beta = \gamma = \frac{1}{2}\pi$, giving

$$\begin{aligned}(T_1')^{-1} = {}& \hbar^{-2}(12A_1^2 + 24\alpha_1^2) \\ & \times\int_0^\infty [\langle S_1^x(t)S_1^x(0)\rangle + \langle S_1^x(t)S_2^x(0)\rangle] \\ & \times\cos\omega_0 t\, dt\,,\end{aligned} \tag{2.20}$$

where T_1' is defined to be the value of T_1 when $\alpha = 0$. Thus the field dependence of $(T_1')^{-1}$ traces out the Fourier transform of the electronic-spin-correlation functions. It should be stressed that this effect is not associated with changes in the NMR frequency, which is much smaller than the electronic-spin-fluctuation rate at all fields; it is due rather to the frequency shift of the transverse electronic-spin-fluctuation spectrum by the applied field, via the factor $\cos\omega_0 t$ in Eq. (2.16).

It is convenient at this point to note several consequences of Eqs. (2.18) and (2.19) which will be useful in the data analysis. First, at zero field $T_1 = T_2$ is independent of α, β, and γ, as must necessarily be the case for cubic symmetry. Second, in the high-field limit the first term in Eq. (2.18) and the last term in Eq. (2.19) both go to zero. One then has

$$\begin{aligned}(T_2^{-1})_{H=\infty}/(T_1^{-1})_{H=0} = {}& [2A_1^2 - 2\alpha_1^2 \\ & + 6\alpha_1^2(\cos^4\alpha+\cos^4\beta+\cos^4\gamma) \\ & + 3\alpha_1^2(2-\sin^4\alpha-\sin^4\beta-\sin^4\gamma)]\end{aligned}$$

$$\times(4A_1^2+8\alpha_1^2)^{-1}. \quad (2.21)$$

Furthermore, again defining T_1' as the value of T_1 when $\alpha=0$, i.e., when the applied field is along the [100] crystalline axis, Eq. (2.18) may be written

$$T_1^{-1} = (T_1')^{-1} \times\left(\frac{2A_1^2-2\alpha_1^2+3\alpha_1^2(\sin^4\alpha+\sin^4\beta+\sin^4\gamma)}{2A_1^2+4\alpha_1^2}\right) + (T_1^{-1})_{H=0}\left(\frac{3\alpha_1^2(2-\sin^4\alpha-\sin^4\beta-\sin^4\gamma)}{2A_1^2+4\alpha_1^2}\right). \quad (2.22)$$

Finally, integration of Eq. (2.20) with respect to ω_0, and noting that $\langle S_i^x(0)S_j^x(0)\rangle=\frac{1}{3}\delta_{ij}S(S+1)$, yields

$$\int_0^\infty (T_1')^{-1}d\omega_0 = 2\pi\hbar^{-2}S(S+1)(A_1^2+2\alpha_1^2). \quad (2.23a)$$

A more general form of this equation can readily be derived by proceeding as before but without the restriction of nearest-neighbor hyperfine coupling only. It is

$$\int_0^\infty (T_1')^{-1}d\omega_0 = 2\pi\hbar^{-2}S(S+1)\frac{1}{6}\sum_i (A_i^2+2\alpha_i^2). \quad (2.23b)$$

The theoretical development has been rigorous up to this point, given the correctness of the assumptions concerning the exchange and hyperfine interactions. However, to proceed further, one must deal with the time dependence of the electronic-spin-correlation functions. This problem has not yielded to an exact calculation for the full-time axis, although a number of workers have obtained approximate solutions.[14] While these various approximate methods agree fairly well, the precise shape of the function is still the subject of some controversy. This is particularly true of the long-time regime.[15] In this paper a relatively simple technique employed by Gulley *et al.*[16] will be used to analyze the data. The assumptions made above about the exchange interaction reduced the present problem to that of the simple-cubic magnet with nearest-neighbor interactions only, so that much of the work by these authors can be taken over directly.

Following Gulley *et al.*[16] we expand Eq. (2.11) in powers of t up to t^4 and then perform the trace prescribed by Eq. (2.13). This yields an even-power series for the correlation functions up to t^4, which we use for $t\leq\omega_{ex}^{-1}$ where

$$\omega_{ex}^2 \equiv \tfrac{2}{3}S(S+1)\hbar^{-2}\sum_{i\neq1}\mathcal{J}_{1i}^2. \quad (2.24)$$

Here ω_{ex}^2 is the coefficient of $\frac{1}{2}t^2$ in the expansion of $\langle S_1^x(t)S_1^x(0)\rangle$, or equivalently, the second moment of the Fourier spectrum of this quantity. For the present study it is perhaps the most suitable parameter with which to characterize the strength of the exchange interactions. In principle the power series could be extended to apply at all times, but in practice the convergence at longer times is very slow and the coefficients rapidly become more difficult to calculate. For $t\geq 2/\omega_{ex}$ we assume that the electronic-spin-correlation functions obey a diffusion equation. The range $\omega_{ex}^{-1} < t < 2\omega_{ex}$ is obtained simply by interpolation. The results for GdP are shown in Fig. 1 for the high-temperature limit.

The autocorrelation function $\langle S_1^x(t)S_1^x(0)\rangle$ has an approximately Gaussian region at short times, with zero slope at the origin. At long times it approaches the $t^{-3/2}$ dependence characteristic of diffusion in three dimensions. The pair correlation function $\langle S_1^x(t)S_2^x(0)\rangle$ is equal to $\frac{1}{6}[\frac{1}{3}S(S+1)-\langle S_1^x(t)S_1^x(0)\rangle]$ at short times, passes through a maximum near $1.8/\omega_{ex}$, and approaches the autocorrelation function at long times. From Eq. (2.18), the contribution to T_1^{-1} in the low-field limit from a given correlation function is proportional to the area under that function. The autocorrelation function obviously dominates, with 4.1 times the area under the pair-correlation function, but the latter cannot be neglected in a quantitative treatment.

It should be noted here that Walstedt[15] has questioned the validity of the long-time behavior assumed by Gulley *et al.*,[16] basing his arguments on the theoretical work of Blume and Hubbard.[17] These authors obtained a set of integrodifferential equations, which they solved numerically for the simple cubic lattice with nearest-neighbor-only exchange. Walstedt further cited the present work[4] to support his position. We will not attempt to judge the relative merits of the Gulley *et al.* approach versus the Blume and Hubbard method, both of which are approximate. However, several points should be made concerning the arguments of Walstedt. First, the low-field T_1 in GdP is substantially affected by the pair-correlation function in Eq. (2.18), and this term has not been included by Walstedt. Second, this author takes the Gulley *et al.* result to be proportional to $t^{-3/2}$ in the range $t\omega_{ex}=2$–10, and notes correctly that the Blume and Hubbard autocorrelation function varies approximately as t^{-2} in the region. However, in reality Gulley *et al.* assumed the form $(t-\omega_{ex}^{-1})^{-3/2}$, which in fact varies approximately as t^{-2} in the above range in general agreement with the Blume and Hubbard results. Nevertheless, significant differences remain between the Gulley *et al.* and the Blume–Hubbard results. As shown in Eq. (2.20), the measured relaxation rate $(T_1')^{-1}$ is proportional to the Fourier transform with respect to time of the spin correlation functions. In Fig. 2 the prediction of the Gulley *et al.* model is given, along with the result when the pair-correlation function is neglected. The importance of the pair term is evident. The Blume–Hubbard calculation, also

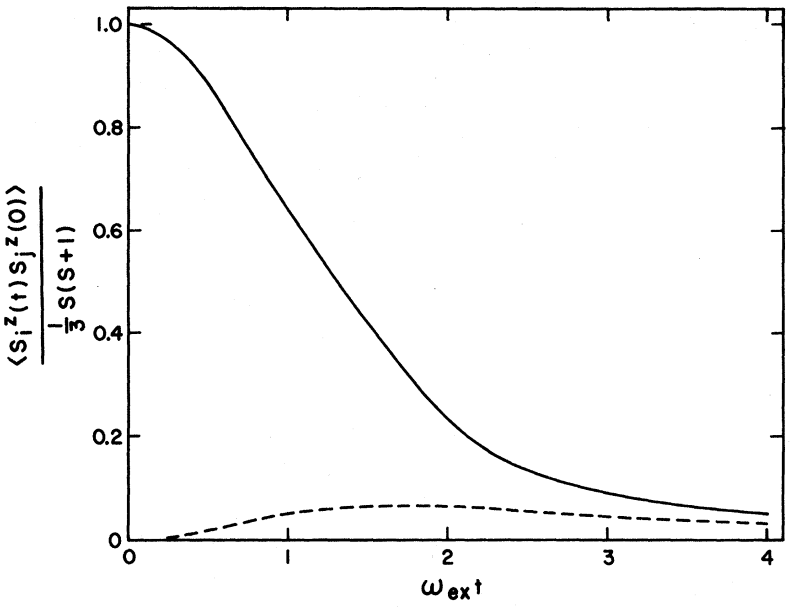

FIG. 1. Electronic-spin-correlation functions, calculated by the method of Gulley *et al.* (Ref. 16) for a simple-cubic antiferromagnet with $S=\frac{1}{2}$ at $T=\infty$. The solid curve gives the autocorrelation function, the dashed curve the nearest-neighbor pair function.

neglecting the pair term, in included for comparison. There is indeed a significant difference, typically around 20%. In particular, as stressed by Walstedt, the calculation of Blume and Hubbard does not exhibit the infinite slope at zero frequency which would be expected from a $t^{-3/2}$ tail in the time domain. Finally, we remark that the agreement between our experimental results and the Gulley *et al.* model is somewhat better than indicated by Walstedt. This point will be discussed in Sec. IV.

Before applying the above theory to GdP, the effect of the classical magnetic dipole-dipole interaction between two Gd spins should be considered. As stated in Sec. I, this coupling is much weaker than the exchange interaction. However, it may nevertheless be significant because, unlike the exchange, it is anisotropic. Hence $\sum_i S_i^z$ does not commute with the electronic-spin Hamiltonian, and as a consequence the decay of the correlation functions at long times will be more rapid than $t^{-3/2}$. An approach due to Richards[18] can be used to estimate the size of this effect. Let the total electronic spin Hamiltonian be written

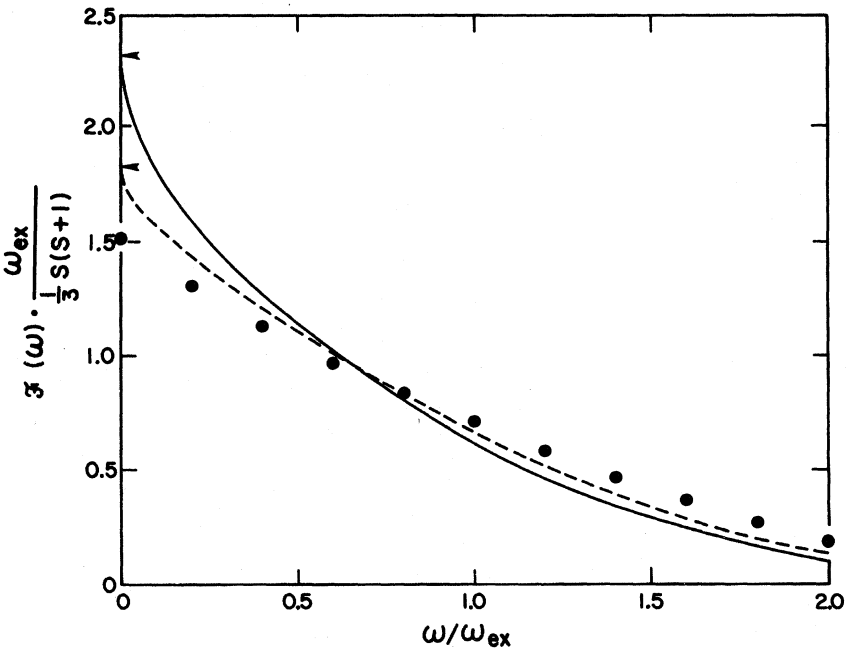

FIG. 2. Normalized Fourier transform of some spin-correlation functions. Solid line, $[\langle S_1^x(t)S_1^x(0)\rangle_\omega + \langle S_1^x(t)S_2^x(0)\rangle_\omega]$ calculated by the method of Gulley *et al.* (Ref. 16); dashed line, $\langle S_1^x(t)S_1^x(0)\rangle_\omega$ alone, using the same method; solid circles, $\langle S_1^x(t)S_1^x(0)\rangle_\omega$ from Blume and Hubbard (Ref. 17). The arrows indicate the $\omega=0$ intercepts for the two curves.

$$\mathcal{H}_{e\,T} = \mathcal{H}_e + \mathcal{H}_D \,, \tag{2.25}$$

where $\mathcal{H}_e$ is given by Eq. (2.2) and

$$\mathcal{H}_D \equiv \tfrac{1}{2}(g\mu_B)^2 \sum_{ij}\left(\frac{\vec{S}_i\cdot\vec{S}_j}{r_{ij}^3} - \frac{3(\vec{r}_{ij}\cdot\vec{S}_i)(\vec{r}_{ij}\cdot\vec{S}_j)}{r_{ij}^5}\right). \tag{2.26}$$

Define three time-dependent spin operators as follows:

$$S^z(t) \equiv e^{+it\mathcal{H}_e/\hbar} S^z e^{-it\mathcal{H}_e/\hbar} \tag{2.27a}$$

(same as Eq. 2.11),

$$\overline{S}^z(t) \equiv e^{+it\mathcal{H}_{eT}/\hbar} S^z e^{-it\mathcal{H}_{eT}/\hbar}\,, \tag{2.27b}$$

and

$$\overline{S}'^z(t) \equiv e^{-it\mathcal{H}_e/\hbar}\,\overline{S}^z(t)\,e^{+it\mathcal{H}_e/\hbar}\,. \tag{2.27c}$$

It can then be readily shown that

$$\langle \overline{S}_i^z(t)\overline{S}_j^z(0)\rangle = \langle S_i^z(t)\overline{S}_j'^z(t)\rangle \tag{2.28}$$

and

$$\frac{d\overline{S}'^z(t)}{dt} = \frac{i}{\hbar}\left[\overline{\mathcal{H}}_D(t),\ \overline{S}'^z(t)\right], \tag{2.29}$$

where

$$\overline{\mathcal{H}}_D(t) \equiv e^{-it\mathcal{H}_e/\hbar}\mathcal{H}_D e^{+it\mathcal{H}_e/\hbar}\,. \tag{2.30}$$

Hence, the effect of the dipolar interaction is to replace $S_i^z(0)$ by $\overline{S}'^z(t)$, whose time dependence is governed by $\overline{\mathcal{H}}_D(t)$. The Hamiltonian $\overline{\mathcal{H}}_D(t)$ is randomly modulated at a rate of the order of ω_{ex}, defined by Eq. (2.24). The problem of the time dependence of $\overline{S}'^z(t)$ then becomes very similar to that of the dipolar linewidth for a system of rapidly moving spins.[19] Proceeding by analogy, $\overline{S}'^z(t)$ will change appreciably in a time of the order of $(\omega_{ex}/\omega_D)\omega_D^{-1}$, thereby causing the correlation functions to decay more rapidly than $t^{-3/2}$. Here ω_D^2 is the Van Vleck second moment associated with the dipolar interaction.[20]

In the present experiment the relevant function is the Fourier transform $\mathcal{F}(\omega)$ of the spin-correlation functions. This will be significantly affected by the dipolar interactions only for frequencies below $(\omega_D/\omega_{ex})\,\omega_D$, with the maximum change occurring at $\omega = 0$. The infinite slope at $\omega = 0$ in Fig. 2 is replaced by a zero slope. $\mathcal{F}(\omega = 0)$ is reduced by an amount which can be estimated simply by truncating the correlation functions in Fig. 1 at the time $(\omega_{ex}/\omega_D)\omega_D^{-1}$; the result is $\Delta\mathcal{F}(\omega = 0)/\mathcal{F}(\omega = 0) \sim -0.4\omega_D/\omega_{ex}$.

III. EXPERIMENTAL TECHNIQUES

The GdP measurements were made on a powdered sample which was used previously in the NMR work of Jones.[3] The three dilute samples were prepared by first arc melting the rare earth metals together. The relative amounts corresponded to $Gd_{0.1}La_{0.9}P_{1.0}$, $Gd_{0.005}La_{0.995}P_{1.0}$, and $Gd_{0.05}Lu_{0.95}P_{1.0}$, respectively. The resulting alloys were ground to powder, mixed with a stoichiometric quantity of phosphorus, and heated under vacuum to 900 °C for approximately four weeks. Subsequent x-ray analysis verified the NaCl structure in all cases. Magnetic fields to 140 kOe could be achieved with a General Electric model K-31505 superconducting solenoid. The sample was thermally isolated from the solenoid by an insert Dewar. With this arrangement sample temperatures below 4 °K could be obtained by pumping on a liquid ^{4}He bath, and 300 °K was maintained with a flow of N_2 gas.

A phase-coherent pulsed-NMR system[21] with $H_1 \simeq 80$ Oe and a frequency range 5–200 MHz was employed for all of the measurements. The low-temperature line shapes and the high-temperature values of T_2 were obtained using the conventional 90°–180° pulse sequence to produce a spin echo. T_1 was measured by the stimulated-echo method,[22] in which a 90°–90°-τ-90° pulse sequence is applied. As the pulse spacing τ increases, the stimulated echo amplitude decreases to zero as $e^{-\tau/T_1}$. This technique was preferable because at 300 °K, T_1 and T_2 were comparable with or shorter than the recovery time of the detection system, and the signal frequently could only be observed after several decay times. The conventional 90°-τ-90°-180° sequence, in which the echo amplitude varies as $[1 - e^{-\tau/T_1}]$,[19] would therefore have necessitated measuring a small difference between two much larger numbers.

Signal averaging was required to obtain satisfactory resolution. In the 300 °K work the signal-to-noise ratio was enhanced by about a factor of 100 in two stages. As the applied field was swept back and forth through resonance, the echo amplitude was monitored with a Princeton Applied Research model CW-1 boxcar integrator. Successive sweeps were accumulated in a Fabri-Tek model 1062 digital computer. The low-temperature work required less averaging, and enhancements of the signal-to-noise ratio as low as 15 were used in some cases.

IV. EXPERIMENTAL RESULTS AND DISCUSSION

A. Line Shapes in LaP:Gd and LuP:Gd

Experimental ^{31}P NMR spin-echo spectra for the nominal $Gd_{0.1}La_{0.9}P_{1.0}$ and $Gd_{0.05}Lu_{0.95}P_{1.0}$ compositions are given in Figs. 3 and 4, respectively. These data were obtained at 2.0 °K and a frequency of 160.00 MHz corresponding to a zero-shift field H_0 of 92.83 kOe. It is reasonable to assume that the observed satellite spectrum corresponds to ^{31}P nuclei having a single Gd nearest neighbor. The nonsymmetric broadening of the satellite is characteristic of anisotropic shift contributions. The observation of only one satellite indicates that the magnitude of the nearest-neighbor Gd-P hyper-

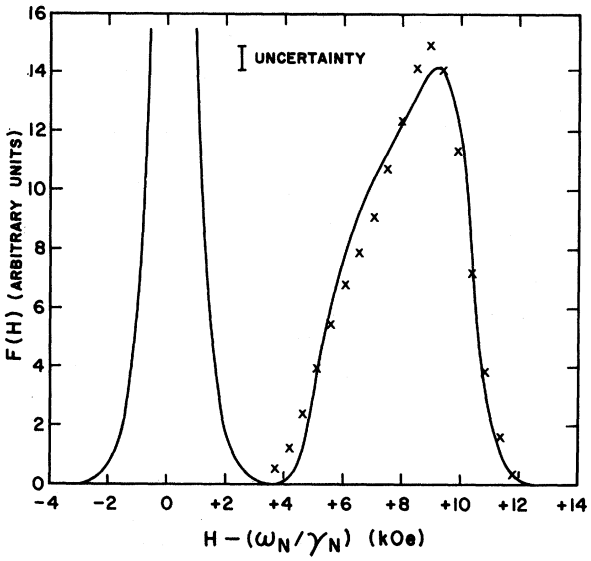

FIG. 3. NMR spectrum for ^{31}P in nominal $Gd_{0.1}La_{0.9}P_{1.0}$ for $T=2$ °K and $\omega_N/\gamma_N=92.83$ kOe. The crosses represent a least-squares fit to Eqs. (4.2) and (4.5) of the text, with fit parameters given in Table I.

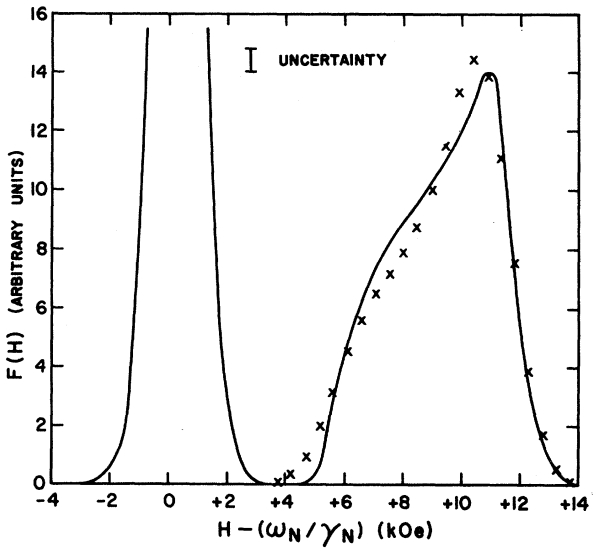

FIG. 4. NMR spectrum for ^{31}P in nominal $Gd_{0.05}Lu_{0.95}P_{1.0}$ for $T=2$ °K and $\omega_N/\gamma_N=92.83$ kOe. The crosses represent a least-squares fit to Eqs. (4.2) and (4.5) of the text, with fit parameters given in Table I.

fine-coupling constant exceeds that of more distant neighbors. The experimental ratio of the area under the satellite to that under the central peak corresponds to a Gd concentration of 0.027 ± 0.005 at.% for the La compound and 0.016 ± 0.003 at.% for the Lu compound. Thus it appears that less than one-third of the starting Gd was incorporated into the dilute compounds.

Under the above experimental conditions, the Gd electronic spins should be almost completely aligned with the applied field. At 2 °K and fields above 93 kOe the Brillouin function $B_{7/2}(g\mu_B H/k_B T)$ is within 0.1% of its maximum value. Furthermore, exchange effects should be negligible at the above concentrations. Two checks on the polarization were made: First, spectra were also obtained for the above La sample at 58 kOe; and second, measurements were made on the nominally $Gd_{0.005}La_{0.995}P_{1.0}$ compound. The width and shift of the satellite did not change. As a consequence of this complete spin polarization (i.e., $\langle S^z\rangle=\frac{7}{2}$), the NMR spectrum depends only on the hyperfine coupling.

In the limit of zero Gd concentration, when each Gd-P nearest-neighbor pair is unaffected by other Gd ions, the satellite line shape is readily calculated. Using Eq. (2.8) and noting that $\vec{S}$ is antiparallel to $\vec{H}$, the component of $\vec{h}$ along $\vec{H}$ is given by

$$h^z=(\gamma_N\hbar)^{-1}\tfrac{7}{2}[-A_1-\mathcal{A}_1(1-3\cos^2\phi)]\,, \qquad (4.1)$$

where ϕ is the angle between $\vec{H}$ and the Gd-P axis. Taking a powder distribution of ϕ then gives the satellite spectrum $F(H)$:

$$\begin{aligned} F(H) &= 0 && \text{if } H<H_1 \\ &= (H_2-H)^{-1/2} && \text{if } H_1<H<H_2 \\ &= 0 && \text{if } H>H_2\,, \end{aligned} \qquad (4.2)$$

where

$$H_1\equiv H_0+(\gamma_N\hbar)^{-1}(A_1-2\mathcal{A}_1)\,, \qquad (4.3)$$

$$H_2\equiv H_0+(\gamma_N\hbar)^{-1}(A_1+\mathcal{A}_1)\,, \qquad (4.4)$$

and H_0 is the center of the central peak. At finite concentrations the interaction of a ^{31}P nucleus with more distant neighbors will broaden the line further. Specifically, the δ function of field which corresponds to any particular value of ϕ will be replaced by a spectrum of finite width. If this spectrum is assumed to have a Gaussian shape, the experimentally observed line shape $F'(H)$ will be given by

$$F'(H)=\int_{-\infty}^{+\infty}F(q)e^{-D^{-2}(q-H)^2}dq\Big/\int_{-\infty}^{+\infty}e^{-D^{-2}(q-H)^2}dq\,, \qquad (4.5)$$

where D is some constant.

Least-squares fits of Eqs. (4.2) and (4.5) to the data are given by the crosses in Figs. 3 and 4.

TABLE I. Parameters from the fits of Eqs. (4.2) and (4.5) to the data in Figs. 3 and 4.

	$A_1/\gamma_N\hbar$ (kOe)	$\mathcal{A}_1/\gamma_N\hbar$ (kOe)	$D/\gamma_N\hbar$ (kOe)
LaP:Gd	2.27 ± 0.20	0.44 ± 0.07	1.35 ± 0.20
LuP:Gd	2.58	0.53	1.30

The resulting values of the parameters are given in Table I. An estimate of the uncertainty in the absolute values of these parameters, based on the data error bars and the quality of the fit, is ± 0.20 kOe for $A_1/\gamma_N\hbar$ and $D/\gamma_N\hbar$, and ± 0.07 kOe for $\mathfrak{a}_1/\gamma_N\hbar$. The variation between samples is known more accurately, and may be expressed in terms of the lattice constants y as $d(\ln A_1)/d(\ln y) = -1.5 \pm 0.4$ and $d(\ln \mathfrak{a}_1)/d(\ln y) = -2.1 \pm 1.0$, where the lattice parameters were given in Sec. I. It should be noted that the value of D is approximately twice the $1/e$-amplitude half-width of the central peak. This may possibly indicate a slight tendency for the Gd ions to cluster, so that the random broadening is greater for P nuclei with Gd nearest neighbors.

The above results may be interpolated to the case of GdP, if it is assumed that A_1 and $\mathfrak{a}_1$ vary lineraly with lattice constant. This is probably an adequate approximation since the total variation of these parameters is less than 20%. One then obtains $A_1/\gamma_N\hbar = 2.46$ kOe and $\mathfrak{a}_1/\gamma_N\hbar = 0.49$ kOe. ^{31}P NMR-shift measurements by Jones[3] in GdP have shown that $\sum_i A_i/\gamma_N\hbar = 19$ kOe. The cubic symmetry prevents a determination of $\mathfrak{a}_1$ from these data. Since the ^{31}P nucleus has six nearest-neighbor Gd ions, the fraction $6A_1/\sum_i A_i = 0.78 \pm 0.05$ of its hyperfine field comes from nearest-neighbor couplings. The remainder is due to longer-range interactions.

Further evidence for the presence of longer-range hyperfine interactions is provided by a shift in the central peak. This peak lies 0.21 ± 0.10 kOe above the zero-shift field $\omega_N/\gamma_N = 92.83$ kOe for the nominal $Gd_{0.1}La_{0.9}P_{1.0}$, and 0.24 ± 0.10 kOe higher for $Gd_{0.95}Lu_{0.95}P_{1.0}$, but 0.08 ± 0.05 kOe lower for the $Gd_{0.005}La_{0.995}P_{1.0}$ sample. This is to be compared with shifts to lower fields of 0.06 ± 0.01 and 0.05 ± 0.01 kOe for LaP and LuP, respectively.[3] The differences may be due to a Gd-P interaction which extends beyond nearest neighbors. Unfortunately, uncertainties associated with the unknown magnitude of sample demagnetization effects makes this interpretation quite tentative.

B. Spin Relaxation Times in GaP

The longitudinal and transverse nuclear-spin-relaxation times T_1 and T_2 were measured for ^{31}P at 300 °K, as a function of applied field up to 115 kOe. Since the ordering temperature is 15 °K, the condition $T \gg T_{\text{Néel}}$ is well satisfied. However, two complications must be dealt with before applying the results of Sec. II. First, it was concluded above that the Gd-P hyperfine coupling extends beyond nearest neighbors, contrary to the assumption made in Sec. II. Second, because the data were taken on a randomly oriented powder, the direction cosines in Eqs. (2.18) and (2.19) are not unique. For nonzero applied fields this results in a distribution of relaxation times and hence in a decay of the total nuclear magnetization which is not exponential in time.

The importance of the longer-range hyperfine couplings in determining T_1 can be estimated by setting both the pair-correlation function $\langle S_1^x(t) S_2^x(0)\rangle$ (Fig. 1) and the anisotropic hyperfine parameters $\mathfrak{a}_1$ to zero. Then, proceeding as in Sec. II, it is straightforward to show that

$$T_1^{-1}(\text{nearest neighbor only})/T_1^{-1} = 6A_1^2/\sum_i A_i^2 \ . \tag{4.6}$$

The magnitude of this ratio depends on the details of the longer-range interactions and cannot be uniquely determined from available information. However, the dominance of the nearest-neighbor term combined with the quadratic dependence of T_1^{-1} on each term leads to the conclusion that the ratio must be very nearly unity. Therefore, it is a reasonable approximation to simply neglect all but the nearest-neighbor couplings A_1 and $\mathfrak{a}_1$.

The effect of making measurements on a randomly oriented powder is to replace the exponential decay function for the longitudinal nuclear magnetization, $M_1(t) = M_1(0)e^{-t/T_1}$, by

$$M_1(t) = (4\pi)^{-1} M_1(0) \int e^{-t/T_1} \, d\Omega \ , \tag{4.7}$$

where $d\Omega$ is the increment of solid angle. A similar modification applies to the transverse decay function $M_2(t) = M_2(0)\, e^{-t/T_2}$. Equations (2.21) and (2.22) express $(T_2^{-1})_{H=\infty}$ and T_1^{-1} in terms of the orientation-independent parameters $(T_1^{-1})_{H=0}$ and $(T_1')^{-1}$, where T_1' was defined to be the value of T_1 when $\vec{H}$ is along the [100] crystallographic axis. Hence, given $A_1/\mathfrak{a}_1$, $(T_1^{-1})_{H=0}$, and $(T_1')^{-1}$, $M_1(t)$ and $M_2(t)_{H=\infty}$ can be calculated. In the case of GdP the anisotropy of T_2 is small at all fields ($\lesssim 4\%$ using the values of A_1 and $\mathfrak{a}_1$ from Sec. IV A). T_1 becomes highly anisotropic only at the highest fields used in our experiments.

The analytical procedure will be to first determine $(T_1^{-1})_{H=0}$ from the high-field decay of the transverse nuclear magnetization $M_2(t)_{H=\infty}$. This is accomplished by assuming a range of values of $(T_1^{-1})_{H=0}$, calculating $M_2(t)$ for each value as described above, and comparing with the data. $(T_1^{-1})_{H=0}$ was not determined directly because at fields < 30 kOe the signal decays became too rapid to measure. Second, the longitudinal decay function $M_1(t)$ will be calculated in the high-field limit where $(T_1')^{-1} = 0$. A refined value of $\mathfrak{a}_1$ will be chosen to produce agreement with experiment. Finally, for each field a value of $(T_1')^{-1}$ will be selected which produces agreement with the longitudinal decay observed experimentally at that field strength. The first step, applied at $H = 115$ kOe where, as will be seen, the high-field limit is very close to

realization, gives $(T_1^{-1})_{H=0} = (1.64 \pm 0.08) \times 10^5$ sec^{-1}.

The observed decay of the longitudinal nuclear magnetization $M_1(t)$ at $H = 115$ kOe is shown in Fig. 5. As will emerge later in the analysis, $(T_1')^{-1}/(T_1^{-1})_{H=0} \simeq 0.0039$ at this field. This difference from the $H = \infty$ limit, where $(T_1')^{-1} = 0$, is small but sufficient to affect $M_1(300\ \mu\text{sec})$ by a few percent. Hence, the first term in Eq. (2.22) cannot be neglected in the calculation of the decay. The dashed line in Fig. 5 was therefore produced numerically using Eqs. (2.22) and (4.7) and the values of $A_1/\mathcal{A}_1$, $(T_1^{-1})_{H=0}$, and $(T_1')^{-1}$ obtained above. In particular, $A_1/\mathcal{A}_1 = 5.0 \pm 1.0$ from Sec. IV A. The improved agreement with the data given by the solid line represents a fit in which $A_1/\mathcal{A}_1$ was allowed to vary, yielding a value of 4.0. From the various uncertainties it is estimated that this ratio has an uncertainty of ± 0.25. Therefore, the present result is consistent with the LaP: Gd and LuP: Gd satellite data. For the remaining analysis $\mathcal{A}_1$ will be changed from 0.49 to 0.62 kOe in order to have $A_1/\mathcal{A}_1 = 4.0$.

The value of $\mathcal{A}_1$ depends on both classical dipolar ($\mathcal{A}_{1,\text{dip}}$) and transferred ($\mathcal{A}_{1,\text{trans}}$) couplings. If the classical contribution, given by Eq. (2.10), is subtracted, one is left with $A_1/\gamma_N\hbar = 2.46$ kOe and $\mathcal{A}_{1,\text{trans}}/\gamma_N\hbar = -0.17$ kOe, which gives $A_1/\mathcal{A}_{1,\text{trans}} = -14.5$. It is interesting to compare this ratio with those for two other systems containing an S-state ion:

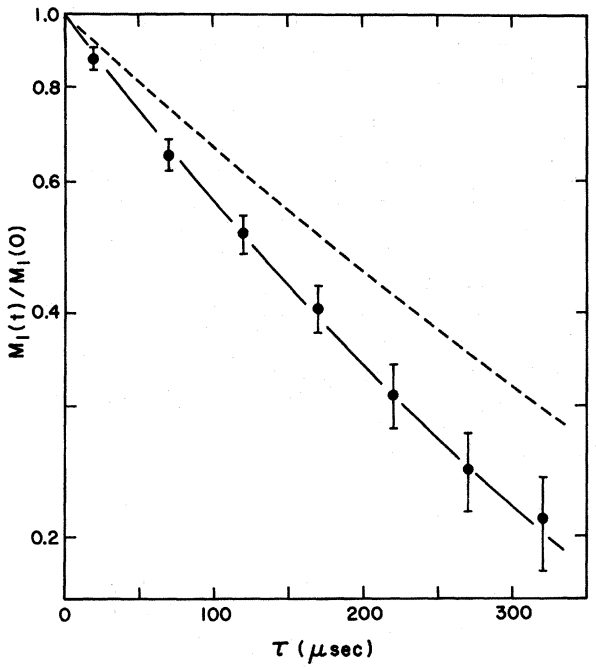

FIG. 5. Decay of the ^{31}P stimulated echo in GdP for $T = 300$ °K and $H = 115$ kOe. The dashed curve is calculated assuming $A_1/\mathcal{A}_1 = 5.0$, the solid line assuming $A_1/\mathcal{A}_1 = 4.0$.

$RbMnF_3$ and $KMnF_3$. One has for the Mn-^{19}F hyperfine coupling $A/\mathcal{A}_{\text{trans}} = -51$ and -96, respectively,[23] using the present notation. These have the same sign as for GdP, but the degree of anisotropy is much smaller.

It should be noted that in the preliminary report[4] on the GdP measurements, published before the low-temperature line shapes in the dilute compounds were available, good consistency was also found among $A_1/\mathcal{A}_1$, $(T_1^{-1})_{H=0}$, and $M_1(t)_{H=115\,\text{kOe}}$. In that case A_1 was obtained from the ^{31}P NMR shift in GdP[3] by incorrectly assuming the hyperfine interaction to be nearest neighbor only. Moreover, $\mathcal{A}_1$ was assumed, also incorrectly, to be due entirely to the classical magnetic dipole-dipole interaction, and was calculated from Eq. (2.10). As a result, while both A_1 and $\mathcal{A}_1$ differed from the present values by about 30%, the fortuitous combination of errors gave $A_1/\mathcal{A}_1 = 4.0$.

The parameter $(T_1')^{-1}$, obtained as described above, is shown as a function of applied field in Fig. 6. The $\log(T_1')^{-1}$-vs-H^2 format was chosen so that a Gaussian dependence would yield a straight line. In order to convey the relative importance of the anisotropy in T_1, the quantity $(4\pi)^{-1}\int (T_1^{-1})_{H=\infty}\, d\Omega$ is given by the horizontal arrow. The solid curve is the Fourier transform of $[\langle S_1^z(t) S_1^z(0)\rangle + \langle S_1^z(t) S_2^z(0)\rangle]$, calculated as in Sec. II, times a constant selected to produce coincidence with the data at $H = 0$. The parameter ω_{ex} [Eq. (2.24)] was adjusted to fit the data above 2×10^{9} Oe^2. Its value is $\omega_{ex} = (7.1 \pm 0.2) \times 10^{11}$ sec^{-1},[24] or in terms of field, $\omega_{ex}/\gamma_e = 40 \pm 1$ kOe.

The two fit parameters used above can be subjected to two consistency checks. First, Eq. (2.23a) gives the area under a $(T_1')^{-1}$-vs-H plot in terms of A_1 and $\mathcal{A}_1$. The area so calculated is smaller than that under the solid curve in Fig. 6 by a factor of 0.94, which is very good agreement. This contrasts with the discrepancy of a factor of 1.7 obtained in Ref. 4, which was due to the incorrect values of A_1 and $\mathcal{A}_1$ which were used. Second, the Curie–Weiss temperature, found by Jones[3] to be -22.4 ± 1.2 °K for GdP, is related to the exchange interactions by[25]

$$\theta = \frac{S(S+1)}{3k_B} \sum_{i \neq 1} \mathcal{J}_{1i} \,. \tag{4.8}$$

Given the assumption of Sec. II that the exchange interaction is next-nearest neighbor only, $\mathcal{J}$ can then be calculated, and from it ω_{ex}. The result is $\omega_{ex} = (7.4 \pm 0.4) \times 10^{11}$ sec^{-1}, in good agreement with the value obtained above. Since Eqs. (2.24) and (4.8) involve respectively a quadratic and a linear sum over $\mathcal{J}_{ij}$, this consistency favors the assumed exchange configuration.

At this point several assertions made earlier can be justified. First, we claimed in Sec. II that

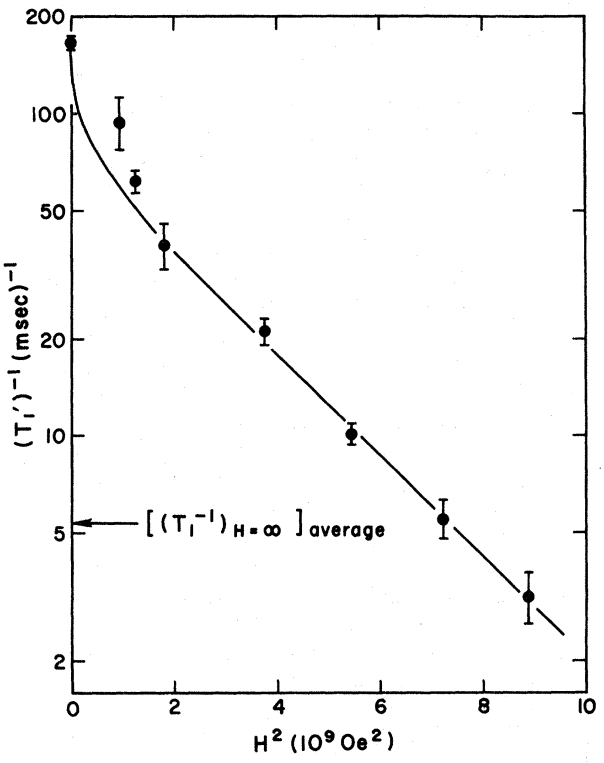

FIG. 6. Magnetic field dependence of $(T_1')^{-1}$ in GdP for $T = 300$ °K. The solid curve is a fit to the spectrum of Gulley *et al.* (Ref. 16), while the horizontal arrow gives the quantity $(4\pi)^{-1}\int (T_1^{-1})_{H=\infty}\, d\Omega$.

nuclear-spin-relaxation mechanisms not associated with Gd spin fluctuations can be neglected. To demonstrate this, two kinds of processes must be considered: spin dephasing produced by the P-P nuclear magnetic dipole-dipole interaction, which affects only T_2, and spin-lattice relaxation, which affects both T_1 and T_2.[12] The Van Vleck second moment[20] for the P-P interaction in GdP is 2.3×10^7 sec^{-2} in angular frequency units. From this, and assuming a Gaussian frequency spectrum and noting that the transverse spin decay function $M_2(t)$ is just the Fourier transform of this spectrum, it can readily be shown that the observed values of T_2 in GdP are changed by less than 0.1%. An estimate of the contribution from spin-lattice relaxation processes was obtained by measuring T_1 at 300 °K in a sample of LaP previously used in the NMR studies of Jones.[3] We found $T_1^{-1} \approx 0.2$ sec^{-1}, which is some 6 orders of magnitude smaller than in GdP. (It should be noted that this value of T_1^{-1} may be determined by rare earth impurities, and therefore larger than for pure LaP. However, for the purposes of the present work, the establishment of an upper bound is obviously quite sufficient.) Second, we assumed that the classical magnetic dipole-dipole interaction between Gd ions can be neglected. Using the results of Sec. II, dipolar effects become important at applied fields below above $\gamma_e^{-1}(\omega_D/\omega_{ex})\omega_D = 0.3$ kOe, ω_D^2 being the Van Vleck second moment.[20] $(T_1^{-1})_{H=0}$ is reduced by a fraction of the order of $0.4\ (\omega_D/\omega_{ex}) = 3\%$. Thus, the assumption seems to be a reasonable one. The final assertion, that $(T_1')^{-1}/(T_1^{-1})_{H=0} \simeq 0.0039$ at $H = 115$ kOe, results from extrapolating the Gaussian tail of the spectrum in Fig. 6 to higher fields.

The detailed shape of the theoretical spectrum in Fig. 6 is in fair agreement with the data, particularly at high fields where both exhibit Gaussian behavior. At lower fields two of the data points fall above the theoretical curve by somewhat more than the experimental uncertainty. Unfortunately, the low-field region is not well characterized experimentally because of the very short relaxation times encountered there. In particular, the divergence of $d(T_1')^{-1}/dH$ at $H = 0$, which is a consequence of the $t^{-3/2}$ tail of the electronic-spin correlation functions in the model of Gulley *et al.*,[16] has not been verified. Also, the area under the experimental $(T_1')^{-1}$-vs-H curve is not well defined if one does not use a theoretical fit as was done above. For example, a smooth curve with zero slope at $\omega = 0$ may be drawn through the data, yielding an area larger than that under the theoretical curve by a factor of 1.3.

V. CONCLUSIONS

The primary objective of this work was to characterize the paramagnetic system GdP. Two different kinds of information were obtained. The first concerned the range and strength of the Gd-P hyperfine interaction and the Gd-Gd exchange interaction, while the second dealt with the dynamics of the electronic-spin system. At least one facet of the study comprised a new method in the study of paramagnets: the determination of electronic-spin-correlation functions directly from the magnetic field dependence of T_1 and T_2.

It was concluded from this study that the nearest-neighbor Gd-P hyperfine interaction (distance = 2.9 Å) is strongest, but that a significant coupling extends at least to next-nearest neighbors (5.0 Å). On the other hand, the Gd-Gd exchange interaction is small for nearest neighbors (4.0 Å), being primarily a next-nearest coupling (5.7 Å). If both interactions are due to conduction-electron polarization,[26] these results suggest a node near 4–5 Å. Such a node would not be inconsistent with the damped oscillatory distribution characteristic of the Ruderman–Kittel–Kasuya–Yosida (RKKY) model.[27] However, contributions from covalent admixture effects typical of nonmetallic systems cannot be ruled out. Indeed, the fact that next-nearest-neighbor Gd ions form an angle of 180°

with an intermediate P ion is suggestive of superexchange.

The theoretically predicted shapes for the electronic-spin correlation functions agreed fairly well with experiment. However, detailed data could not be obtained in the low-field region where the $t^{-3/2}$ diffusion tail[14] would be most clearly exhibited. Diffusive spin behavior has been observed in one dimension, where the correlation functions go as $t^{-1/2}$ at long times, via EPR.[28] However, to our knowledge a definitive experimental result has not been obtained for the autocorrelation function in the three-dimensional case. Furthermore, the predicted magnitude of the $t^{-3/2}$ tail has been questioned.[15] It would therefore seem very desirable to apply the techniques developed in this work to a system in which the low-field range is experimentally more accessible than in GdP.

Note added in proof. Reiter has independently carried out a more detailed treatment of the effect of dipolar coupling on the electronic spin correlation function than that presented in Sec. II [G. Reiter, Phys. Rev. B (to be published)]. In particular, his findings confirm that $\Delta\mathcal{F}(\omega=0)/\mathcal{F}(\omega=0)\propto\omega_D/\omega_{ex}$.

ACKNOWLEDGMENTS

The authors are indebted to Dr. R. K. Quinn for supplying the dilute Gd samples, and to Dr. R. R. Bartkowski and Dr. P. M. Richards for permission to quote unpublished results. They acknowledge helpful conversations with these colleagues as well as with Dr. E. D. Jones, Dr. G. Reiter, and Dr. B. G. Silbernagel. The valuable technical assistance of D. C. Barham is also gratefully acknowledged.

---

*Work supported by the U.S. Atomic Energy Commission.

[1]A preliminary report of this work was given in Ref. 4.

[2]See, for example, A. Tucciarone, J. M. Hastings, and L. M. Corliss, Phys. Rev. Lett. **26,** 257 (1971).

[3]E. D. Jones, Phys. Rev. **180,** 455 (1969).

[4]S. M. Myers and A. Narath, Phys. Rev. Lett. **27,** 641 (1971).

[5]S. M. Myers and A. Narath, Bull. Am. Phys. Soc. **16,** 315 (1971); Bull. Am. Phys. Soc. **17,** 310 (1972); and unpublished.

[6]The electrical resistivities of GdP, DyP, and TbP have been measured by K. Yaguchi [J. Phys. Soc. Jap. **21,** 1226 (1966)] and a ^{31}P NMR Knight shift was reported in Ref. 3 for the nonmagnetic compounds LaP and LuP.

[7]R. R. Bartkowski (private communication).

[8]G. Busch, P. Schwob, O. Vogt, and F. Hulliger, Phys. Lett. **11,** 100 (1964).

[9]E. D. Jones and B. Morosin, Phys. Rev. **160,** 451 (1967). Note that the value of the Curie–Weiss temperature has been revised in Ref. 3 to -22.4 °K. The exchange ratio of 4 given in the text comes from using the latter value in the molecular-field analysis.

[10]See, for example, *Landolt–Bornstein Numerical Data and Functional Relationships in Science and Technology* (Springer-Verlag, New York, 1971), Group III, Vol. 6.

[11]R. R. Bartkowski, *Proceedings of the Seventeenth Annual Conference on Magnetism and Magnetic Materials, 1971*, edited by C. D. Graham, Jr. and J. I. Rhyne (AIP, New York, 1972), p. 1174.

[12]See, for example, C. P. Slichter, *Principles of Magnetic Resonance* (Harper and Row, New York, 1963).

[13]T. Moriya, Prog. Theor. Phys. **16,** 23 (1956).

[14]See, for example, Refs. 15–17 and references therein.

[15]R. E. Walstedt, Phys. Rev. B **5,** 3782 (1972).

[16]J. E. Gulley, D. Hone, D. J. Scalapino, and B. G. Silbernagel, Phys. Rev. B **1,** 1020 (1970).

[17]M. Blume and J. Hubbard, Phys. Rev. B **1,** 3815 (1970).

[18]P. M. Richards (private communication).

[19]See, for example, A. Abragam, *The Principles of Nuclear Magnetism* (Oxford U. P., London, 1961).

[20]J. H. Van Vleck, Phys. Rev. **74,** 1168 (1948).

[21]A. Narath and D. C. Barham (unpublished).

[22]E. L. Hahn, Phys. Rev. **80,** 580 (1950).

[23]M. B. Walker and R. W. H. Stevenson, Proc. Phys. Soc. Lond. **87,** 35 (1966).

[24]This value of ω_{ex} is slightly different from the result $\omega_{ex}=(7.0\pm0.2)\times10^{11}$ sec^{-1} reported in Ref. 4. The change is a consequence of the more refined analysis in the present work.

[25]See, for example, J. H. Van Vleck, *The Theory of Electric and Magnetic Susceptibilities* (Oxford U. P., London, 1965), Chap. 12. Note that in this reference J is defined to be the exchange integral, while we have defined $\mathcal{J}$ to be twice the exchange integral.

[26]See, for example, Ref. 3.

[27]See, for example, C. Kittel, *Quantum Theory of Solids* (Wiley, New York, 1963), Chap. 18.

[28]R. E. Dietz, F. R. Merritt, R. Dingle, D. Hone, B. G. Silbernagel, and P. M. Richards, Phys. Rev. Lett. **26,** 1186 (1971).